Supplementary Documents: Section A (Particle Size)

1. Particle size distribution

The particle size distribution for both precursors is given in Figure S1. Particle size analysis showed that the zeolite sample had particles ranging from 0.3 to 200 microns in size with a D_v (90) of 54.2µm and showed two peaks: one around 0.8 microns and another about 45 microns. The particle size of the BFS sample was in the range of 0.2 to 100 microns (D_v (90): 35 µm), and similar to zeolite, it exhibited two peaks: one peak around 0.5 microns and one about 20 microns.

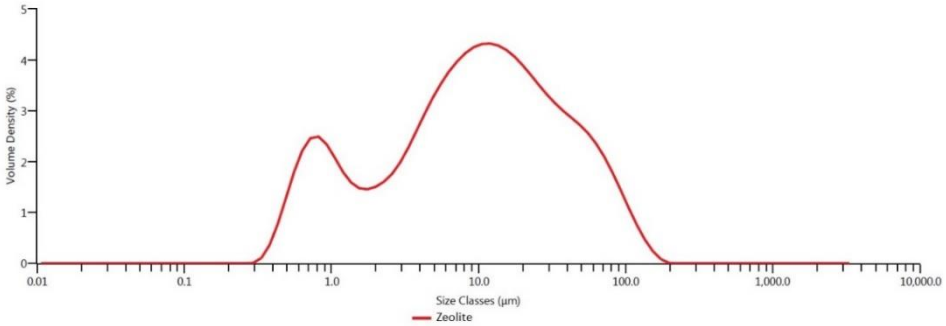

(**a**)

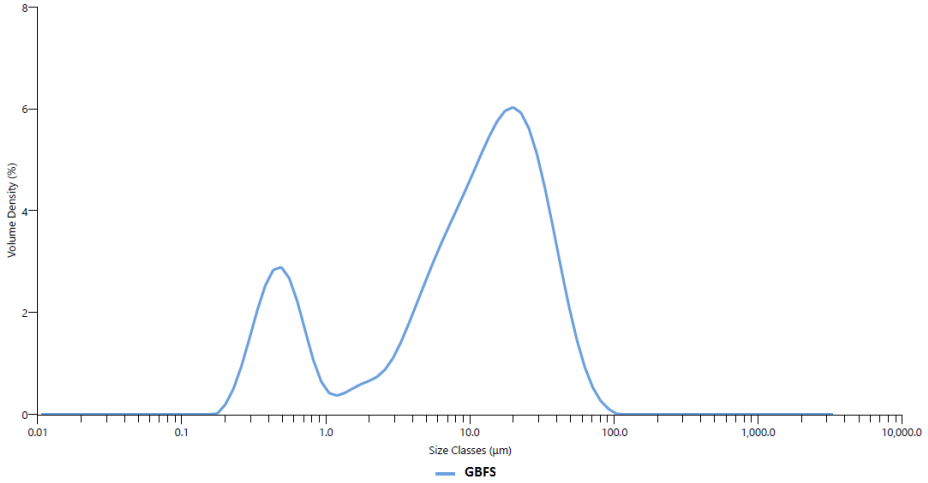

(**b**)

Figure S1. The particle size distribution of (a) zeolite and (b) BFS.

Supplementary Documents: Section B (X-ray Diffraction Quantitative Data)

Corundum	11.11
Quartz	7.31
Calcite	0.73
Gypsum	1.76
Sodium Carbonate Hydrate	1.1
Plagioclase (Albite)	0.52
Plagioclase (Andesine, An50, C1structure)	1.58
Plagioclase (Anorthite)	0.69
K-Feldspar (Orthoclase)	1.53
K-Feldspar (Sanidine, Na0.07)	1.49
Clinoptilolite-Ca	2.34
Clinoptilolite-Na	2.64
Heulandite	1.54
Mordenite	1.2
Stilbite	1.56
Zeolite A	0.86
Zeolite X, Na Exchanged	0.08
Zeolite P	0.01
Kilchoanite, syn	0.11
Amorphase phase	72.95

Corundum	11.11
Quartz	6.85
Calcite	1.97
Gypsum	1.91
Sodium Carbonate Hydrate	0.88
Plagioclase (Albite)	0.4
Plagioclase (Andesine, An50, C1structure)	1.46
Plagioclase (Anorthite)	0.75
K-Feldspar (Orthoclase)	1.59
K-Feldspar (Sanidine, Na0.07)	2.34
Clinoptilolite-Ca	1.27
Clinoptilolite-Na	2.84
Heulandite	0.97
Mordenite	0.56
Stilbite	1.36
Zeolite A	1.24
Zeolite X, Na Exchanged	0.14
Zeolite P	0.07
Kilchoanite, syn	0
Amorphase phase	73.42

Corundum	11.11
Quartz	3.57
Calcite	1.98
Gypsum	2.21
Sodium Carbonate Hydrate	3.38
Plagioclase (Albite)	2.57
Plagioclase (Andesine, An50, C1structure)	1.98
Plagioclase (Anorthite)	1.64
K-Feldspar (Orthoclase)	0.63
K-Feldspar (Sanidine, Na0.07)	1.21
Clinoptilolite-Ca	0.9
Clinoptilolite-Na	2.61
Heulandite	0.7
Mordenite	0.51
Stilbite	3.28
Zeolite A	1.66
Zeolite X, Na Exchanged	0.02
Zeolite P	0.97
Kilchoanite, syn	0
Amorphase phase	70.18

20%BFS-25°C-28days	**Aug-19**
Corundum	11.11
Quartz	9.95
Calcite	0.6
Gypsum	1.66
Sodium Carbonate Hydrate	1.46
Plagioclase (Albite)	1.09
Plagioclase (Andesine, An50, C1structure)	1.31
Plagioclase (Anorthite)	4.66
K-Feldspar (Orthoclase)	0.95
K-Feldspar (Sanidine, Na0.07)	2.05
Chabazite	0.3
Clinoptilolite-Ca	0.62
Clinoptilolite-Na	0.47
Heulandite	0
Mordenite	0.47
Stilbite	1.37
Zeolite A	0.91
Zeolite X, Na Exchanged	0.2
Zeolite P	0.38
Non-diffracting/unidentified	71.56

20%BFS-40°C-28days	**Aug-19**
Corundum	11.11
Quartz	8.93
Calcite	0.07
Gypsum	0.39
Sodium Carbonate Hydrate	1.91
Plagioclase (Albite)	2.11
Plagioclase (Andesine, An50, C1structure)	2.51
Plagioclase (Anorthite)	1.41
K-Feldspar (Orthoclase)	0.99
K-Feldspar (Sanidine, Na0.07)	1.84
Chabazite	0.22
Clinoptilolite-Ca	0.82
Clinoptilolite-Na	1.05
Heulandite	0.2
Mordenite	0.46
Stilbite	2.22
Zeolite A	1.08
Zeolite X, Na Exchanged	0.09
Zeolite P	0.64
Non-diffracting/unidentified	73.07

20%BFS-60°C-28days	**Aug-19**
Corundum	11.11
Quartz	3.66
Calcite	0.13
Gypsum	2.5
Sodium Carbonate Hydrate	9.67
Plagioclase (Albite)	1.54
Plagioclase (Andesine, An50, C1structure)	1.69
Plagioclase (Anorthite)	1.07
K-Feldspar (Orthoclase)	1.11
K-Feldspar (Sanidine, Na0.07)	1.81
Chabazite	1.69
Clinoptilolite-Ca	0.68
Clinoptilolite-Na	1.74
Heulandite	0.55
Mordenite	0.32
Stilbite	1.15
Zeolite A	0.73
Zeolite X, Na Exchanged	0.03
Zeolite P	0.31
Non-diffracting/unidentified	69.62

10%BFS-25°C-28days	**Aug-19**
Corundum	11.11
Quartz	11.26
Calcite	0.15
Gypsum	0.31
Sodium Carbonate Hydrate	2.66
Plagioclase (Albite)	1.27
Plagioclase (Andesine, An50, C1structure)	2.04
Plagioclase (Anorthite)	0.79
K-Feldspar (Orthoclase)	1.26
K-Feldspar (Sanidine, Na0.07)	2.54
Chabazite	0.42
Clinoptilolite-Ca	2.44
Clinoptilolite-Na	2.23
Heulandite	0.32
Mordenite	0.98
Stilbite	1.04
Zeolite A	0.86
Zeolite X, Na Exchanged	0.24
Zeolite P	0.18
Non-diffracting/unidentified	68.99

10%BFS-40°C-28days	**Aug-19**
Corundum	11.11
Quartz	10.26
Calcite	0.1
Gypsum	0.3
Sodium Carbonate Hydrate	2.51
Plagioclase (Albite)	1.53
Plagioclase (Andesine, An50, C1structure)	2.41
Plagioclase (Anorthite)	1.3
K-Feldspar (Orthoclase)	0.97
K-Feldspar (Sanidine, Na0.07)	2.24
Chabazite	0.32
Clinoptilolite-Ca	1.96
Clinoptilolite-Na	1.69
Heulandite	0
Mordenite	0.26
Stilbite	1.59
Zeolite A	1.09
Zeolite X, Na Exchanged	0.16
Zeolite P	0.43
Non-diffracting/unidentified	70.87

10%BFS-60°C-28days	**Aug-19**
Corundum	11.11
Quartz	7.3
Calcite	0.23
Gypsum	0.65
Sodium Carbonate Hydrate	12.24
Plagioclase (Albite)	1.01
Plagioclase (Andesine, An50, C1structure)	1.43
Plagioclase (Anorthite)	0.65
K-Feldspar (Orthoclase)	0.99
K-Feldspar (Sanidine, Na0.07)	2.5
Chabazite	1.46
Clinoptilolite-Ca	1.18
Clinoptilolite-Na	2.9
Heulandite	0.46
Mordenite	0.77
Stilbite	0.94
Zeolite A	0.78
Zeolite X, Na Exchanged	0.08
Zeolite P	0.26
Non-diffracting/unidentified	64.17

BFS	**Aug-19**
Corundum	11.11
Calcite	0.49
Gypsum	5.06
Kilchoanite, syn	0.07
Amorphase phase	94.39

Figure S2. XRD quantitative data for mined zeolite/BFS composite with BFS contents of 10%, 20%, 30% and BFS.

Crystals	PDF #	Formula
Corundum	98-000-0174	Al2O3
Quartz	98-000-0369	SiO2
Calcite	99-002-0010	CaCO3
Gypsum	01-074-1905	Ca(SO4)(H2O)2
Sodium Carbonate Hydrate	01-072-7992	Na2(CO3)(H2O)10.04
Plagioclase (Albite)	01-075-1142	NaAlSi3O8
Plagioclase (Andesine, An50, C1structure)	05-001-0801	$Na_{0.51}Ca_{0.49}(Si_{2.56}Al_{1.44}O_8)$
Plagioclase (Anorthite)	00-012-0301	CaAl2Si2O8
K-Feldspar (Orthoclase)	00-019-0931	K Al Si3 O8
K-Feldspar (Sanidine, Na0.07)	00-010-0353	K Al Si3 O8
Clinoptilolite-Ca	00-039-1383	K Na2 Ca2 (Si29 Al7) O72 ·24 H2 O
Clinoptilolite-Na		
Heulandite		
Mordenite		(Ca, Na2, K2)Al2Si10O24·7H2O
Stilbite		NaCa4(Si27Al9)O72·28(H2O
Zeolite A	00-011-0590	Al12 H54 Na12 O75 Si12
Zeolite X, Na Exchanged	01-074-2512	Al88 Na88 O384 Si104
Zeolite P	04-011-3347	Al3.6 H28 Na3.6 O46 Si12.4
Kilchoanite, syn	04-009-7055	Ca6 O14 Si4
Chabazite	01-088-1263	$Ca_{1.76}\ Al_{3.60}\ Si_{8.40}\ O_{24}\ (\ H_2\ O\ )_{9.87}$

Figure S3. Name, formula and PDF number of crystalline phases found in alkali-activated samples.

Supplementary Documents: Section C (EDS)

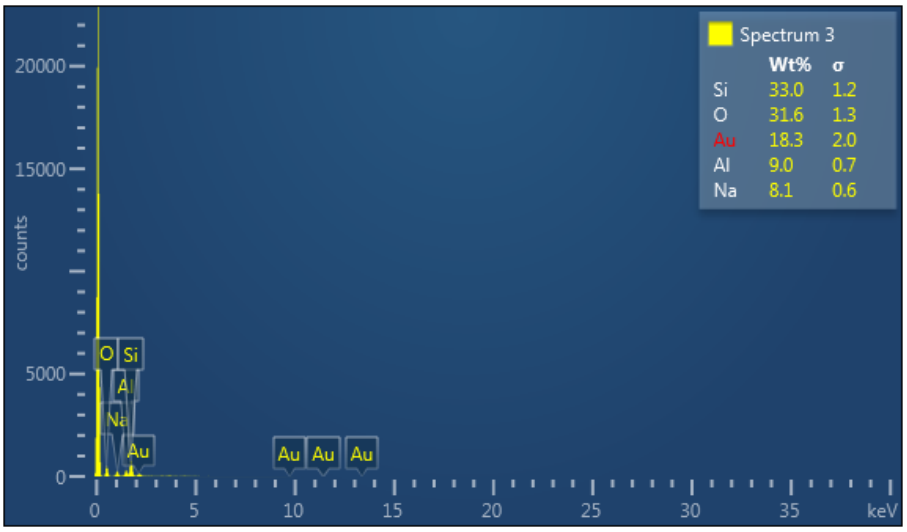

Figure S4. EDS results of zeolite P.

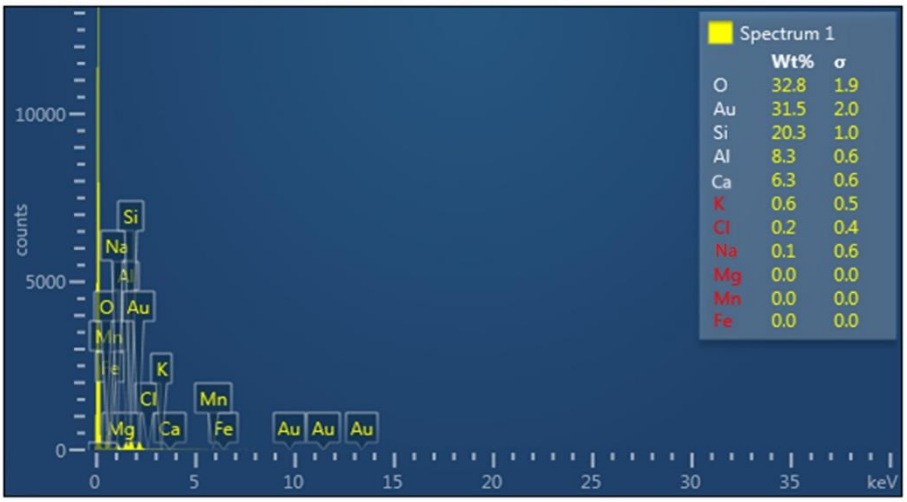

Figure S5. EDS results of Ca-chabazite crystals.

Supplementary Documents: Section D (NMR Quantitative Data)

Table S1. Data extracted from ^{29}Si NMR spectra of zeolite, BFS and geopolymer samples.

Sample	Si/Al *	Q^0		Q^1(1Al)		Q^1(0Al)		Q^2(1Al)		Q^4 (3Al)		Q^4 (2Al)		Q^4 (1Al)		Q^4 (0Al)	
		δ (ppm)	**Area (%)**	**δ (ppm)**	**Area (%)**	**δ (ppm)**	**Area (%)**	**δ (ppm)**	**Area (%)**	**δ (ppm)**	**Area (%)**	**δ (ppm)**	**Area (%)**	**δ (ppm)**	**Area (%)**	**δ (ppm)**	**Area (%)**
Zeolite	4.6	-	-	-	-	-	-	-	-	-	-	−94	6.7	−100 −107	45.5 43.2	−112	4
0%BFS−60°C	3	-	-	-	-	-	-	-	-	−88.82	7.9	−95	19	−101 −107	40.4 31.1	−112	1.5
30%BFS−25°C	3.74	−73.54 −71.23	0.4 0.5	−74.89	0.5	−78.44	4.7	−85.26 −82.21	21.6 15.2	-	-	−91.09	27.1	−101 −107	11.8 17.4	−112	0.7
30%BFS−40°C	3.47	-	-	−74.64	0.3	-	-	−83.21 −85.58	32.5 10.3	−90.24	24.8	−98.1 −95.7	0.3 8.5	−101 −107	8.4 14.5	−112	0.3
30%BFS−60°C	3.11	−73.93 −71.97	0.2 0.5	-	-	−79.51 −76.03	3.21	−83.39 −85.46 −87.02	10.4 2.3 17.4	−92.01	26.5	−97.43	12.2	−101 −107	19.4 5.1	−111	1.7

* Si/ Al ratio calculated using Eq.S1.

Table S2. Quantitative analyses of the ^{27}Al NMR spectra of zeolite, BFS and geopolymer samples.

Sample	Al (IV) (%)	Al (VI) (%)	Al (V) (%)	$(Si/Al)_{fr}$*	(Si/Al) atomic
Mined Zeolite	98	2	0	5	4.9
0%BFS	96.9	3.1	0	6.48	6.28
BFS	100	0	0	2.14	2.14
30%BFS−25°C	96.9	3.1	0	4.43	4.3
30%BFS−40°C	92.9	1.7	5.4	4.62	4.29
30%BFS−60°C	98.8	1.2	0	4.34	4.28

*$(Si/Al)_{fr}$ was calculated using $(Si/Al)_{fr} = (Si/Al)_{total}$ $(I_{55} + I_0)/I_{55}$, in which I_{55} and I_0 are the integrated area intensities of signals at 55 and 0 ppm.

Supplementary Documents: Section E (^{27}Al NMR Spectra)

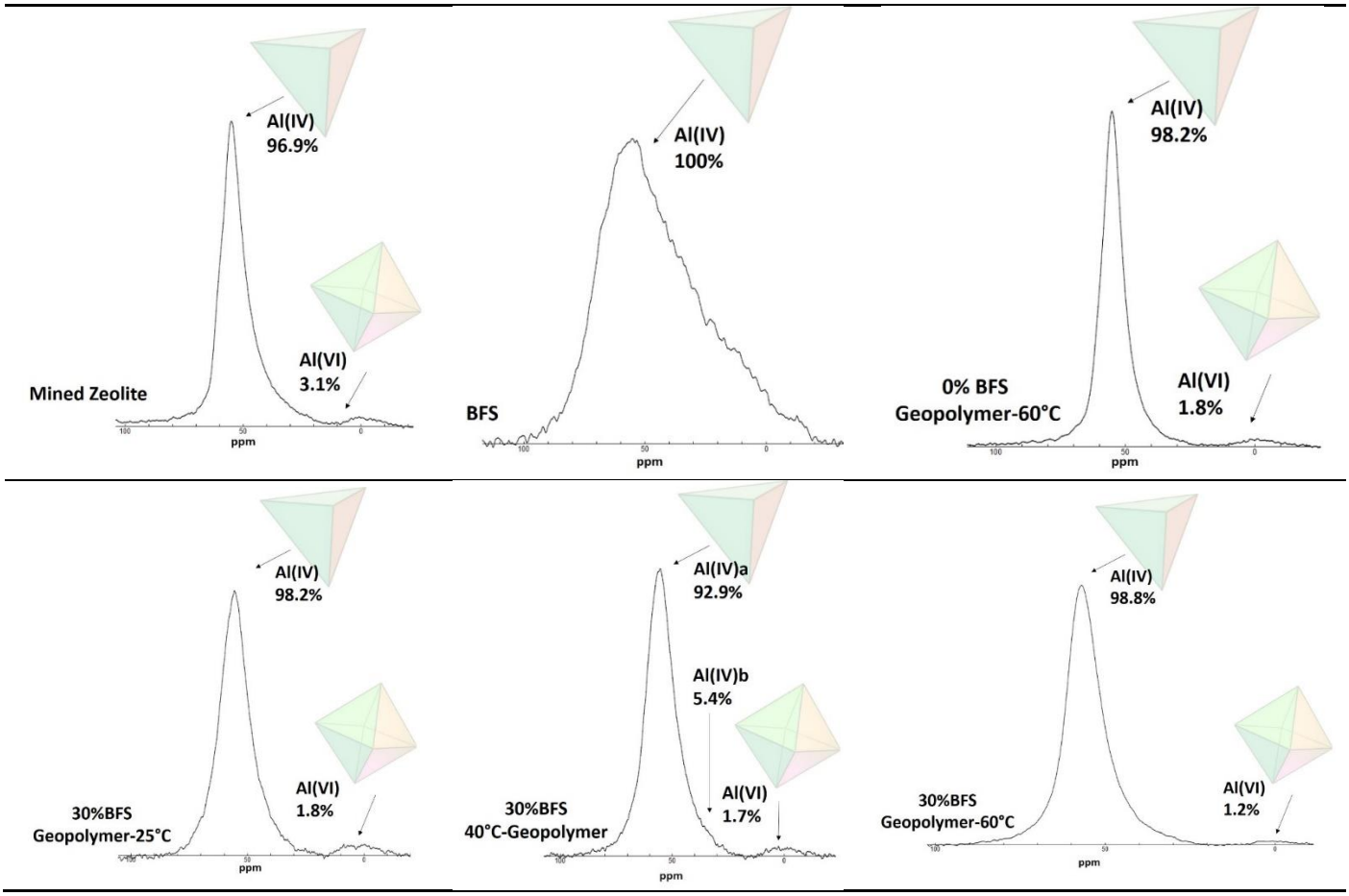

Figure S6. ^{27}Al NMR Spectra for mined zeolite, BFS and geopolymer samples with 30% BFS cured at different temperatures.

Supplementary Documents: Section F

Molecular Structure Study of Zeolite, BFS and Geopolymers

To study the molecular structure, purity and content of starting materials and geopolymers, solid-state NMR experiments were performed. ^{29}Si is the most broadly studied nucleus of mineralogical attention. Silicates are generally categorised based on the way the silicate polyhedra are linked and the degree of polymerisation. The ^{29}Si chemical shift in NMR spectroscopy is sensitive to coordination number, type of coordination, tetrahedral framework atom and degree of polymerisation. Consequently, the molecular structure of minerals can be predicted using ^{29}Si NMR analyses. The newest NMR studies used ^{29}Si and ^{27}Al to study the local structure of aluminosilicate-based precursors like geopolymers, sol-gel materials and minerals[48]. Applying information collected from ^{29}Si NMR analyses aids in finding the Si/Al ratio of minerals using Eq. (S1)[49]..

$$Si/Al = \sum I_{n,m} / \sum (m/n) I_{n,m} \quad \text{(S1)}$$

where n is the number of Si-O-T (T: Si or Al) bridges, m is the number of Si-O-Al bonds and $I_{n,m}$ is the intensity of the $Q^n(m\text{Al})$ peaks. $Q^n(m\text{Al})$ is utilised to define the link of a silicon tetrahedron bridged via oxygen to aluminium and other silicon cores. This notation is generally applied for characterising aluminosilicate systems including zeolites and geopolymers. Note: Eq.S1 only considers the Al of the tetrahedral framework and neglects non-framework Al[49]. It is believed in geopolymer systems that all silicon and aluminium sites are in tetrahedral coordination and n is equal to 4 [50] similar to zeolites; thus, when zeolites are incorporated in geopolymer assembly, tracking structure changes using ^{29}Si NMR spectra is a challenging course.

Figure S7 shows ^{29}Si NMR spectra for the zeolite, BFS and geopolymers after deconvolution. The ^{29}Si NMR of mined zeolite (Figure S7a) presented four peaks according to the different Si locations within the framework which were represented by resonance around −94 ppm, −100 ppm, −107 ppm and −112 ppm, assigned to Q^4(2Al), Q^4 (1Al), Q^4(1Al) and Q^4(0Al), respectively[48-51]. There was also a small peak at around −97 ppm which was associated with the presence of Fe^{3+} species within the framework [51]. This peak also overlapped with the peak at −94 ppm [51]. The Si/Al ratio of mined zeolite was found to be 4.6 using Eq.S1, which was comparable with the number attained by XRF analysis. In the ^{29}Si NMR of unreacted BFS (Figure S7b), the resonance around −75 ppm was representative of the resonance for akermanite glass (Q^1) and solid solutions of gehlenite glass, i.e., Q^2(2Al).

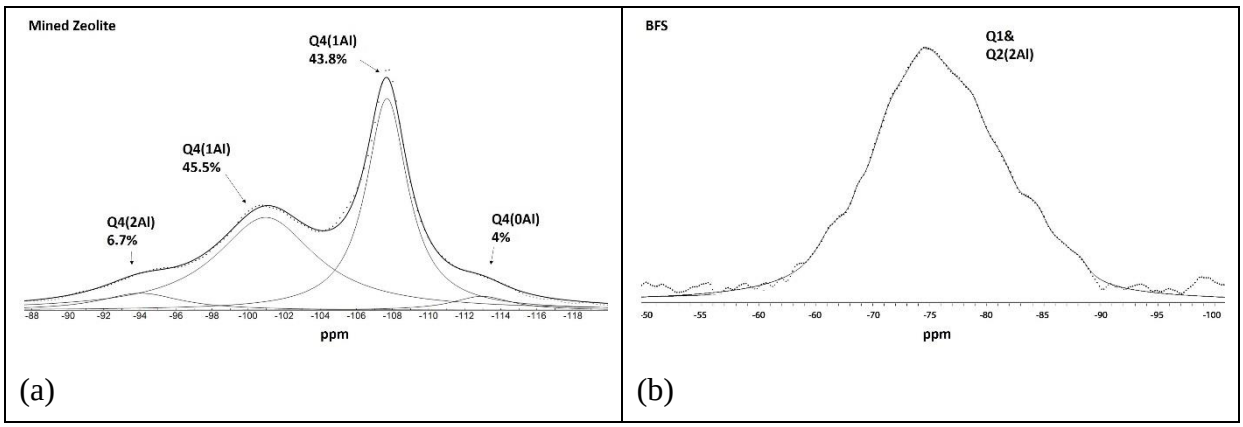

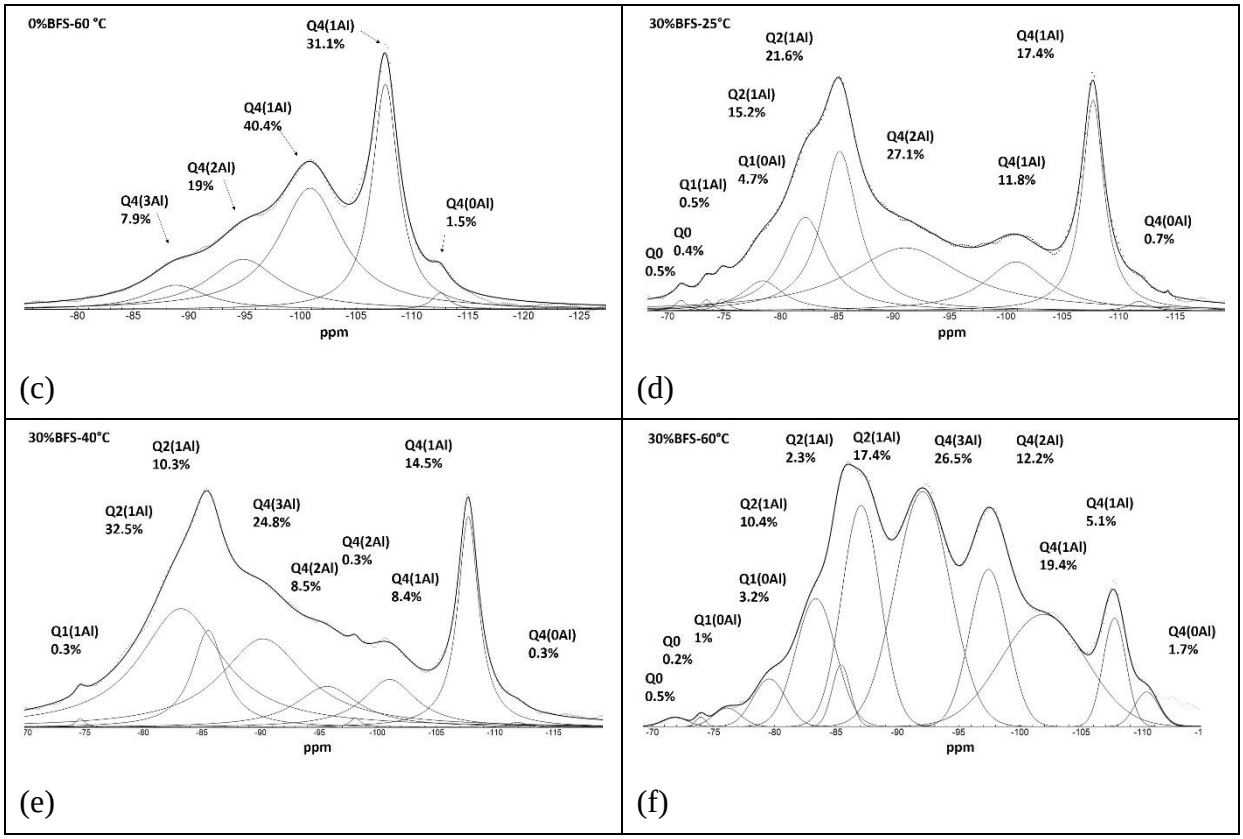

Figure S7. SP-MAS ^{29}Si NMR spectrum and corresponding analytical fit of mined zeolite, BFS and geopolymer composites with 30% BFS and cured at 25, 40 and 60°C.

Although the ^{29}Si NMR spectra of geopolymerised zeolite with no BFS addition (Figure S7c) were found to be similar to that of fresh zeolite, the geopolymer not only displayed more broad spectra, but also there were small differences such as the formation of a peak at around −88 ppm which was the resonance from unreacted oligomers[13]. This peak could also be assigned to Q^4 (3Al). Other changes were the low-field shift of the peaks at −94 ppm and −100 ppm to −95 ppm and −101 ppm, respectively. This peak shift behaviour could be because of the Al-induced next-nearest-neighbour effects in which the structure remains unchanged[13]. Another dissimilarity in the spectra was the change in intensity (or integrated peak area), which was associated with the number of the respective resonance atoms[49]. The lower peak intensity at −112 ppm, −101 and −107 ppm suggested the presence of Q^4 (0,1Al) units, indicating the occurrence of the dissolution and consumption of zeolite. However, the higher intensity of the peak at −95 ppm suggested a higher formation of Q^4 (2Al), proving the development of geopolymerisation in the sample[13].

Figure S7d displays the ^{29}Si NMR spectra of sample ZS30–25°C. As can be seen, a peak shift occurred at around −79 ppm which allocated the hydrated Q^1 units of akermanite, a strong peak at −82 ppm was formed which was assigned to hydrated Q^2(1Al) units of gehlenite, and small resonances at around −75 ppm were related to the unreacted BFS. Peaks discussed so far are related to the alkali activation of BFS and are not yet considered as the three-dimensional geopolymer structure. A peak at −85 ppm arose, inferred to be related to the Q^2(1Al) units, and broad resonances at around −91 ppm suggest the formation of Q^4(2Al) units. The peaks at −100 ppm, −107 ppm and −112 ppm are similar to peaks observed in the NMR spectra of mined zeolite, yet with lower intensities. Moreover, the intensity of peaks at −95 ppm and −97 ppm decreased, showing a reduction in Q^4(3Al) units and Fe^{3+} species. No major change was observed in the ^{29}Si NMR spectra by increasing the curing temperature from 25°C to 40°C (Figure S7e). However, small differences such as the lower intensity of some peaks were detected. The peak intensity of −112 ppm,

−107 ppm and −101 ppm peaks was reduced, indicating the lower content of Q^4(0Al) and Q^4(1Al) units. Meanwhile, broad resonances between −90 and −95 ppm appeared, indicating the greater formation of Q^4 (2Al) and Q^4 (3Al) units. Increasing the curing temperature to 60°C (Figure S7f) resulted in critical changes to ^{29}Si NMR spectra. The spectra were found to be broader and more featureless, which proved the successful formation of geopolymer gel[13]. The new peaks formed at −97 ppm, −92 ppm and −87 ppm, which were assigned to Q^4 (2Al) and Q^4 (3Al) units and not fully reacted oligomers. Compared to the sample prepared at 40°C, the intensities of the peaks at around −111 ppm and −97 ppm increased, approving the production of Q^4(0Al) and Q^4(2Al) units. Intensity reduction of the peaks at −83 ppm and −85 ppm and intensity growth of the peak at −87 ppm happened at almost the same degree, showing that oligomers and monomers were changing from one form to another by changing the curing temperature.

The ^{27}Al NMR spectra of mined zeolite, BFS and their corresponding geopolymers. In the ^{27}Al NMR spectrum of mined zeolite (supplementary section), two peaks were detected, one at 55 ppm and another at 0 ppm, which were related to tetrahedrally coordinated aluminium (i.e., Al^{IV}) and extra-framework octahedral coordinated aluminium (i.e., Al^{VI} species) respectively[51]. The Al^{IV}/Al^{VI} ratio in mined zeolite was found to be around 48 and geopolymerisation reduced this ratio to about 31. These data show that the amount of extra-framework octahedral Al was increased in the geopolymer sample. After adding 30% BFS and geopolymerisation for 28 days at room temperature, this ratio showed a small increase, indicating a minor reduction in octahedral Al compared to the sample prepared with no BFS. By increasing the temperature to 40°C, a peak at around 35 ppm arose that was related to penta-coordinated Al species[52]. Further increasing the temperature to 60°C resulted in a substantial increase in the Al^{IV}/Al^{VI} ratio[51]. Quantitative data extracted from ^{29}Si and ^{27}Al NMR spectra of zeolite, BFS and geopolymers are collected in the supplementary section.

Section G (FTIR)

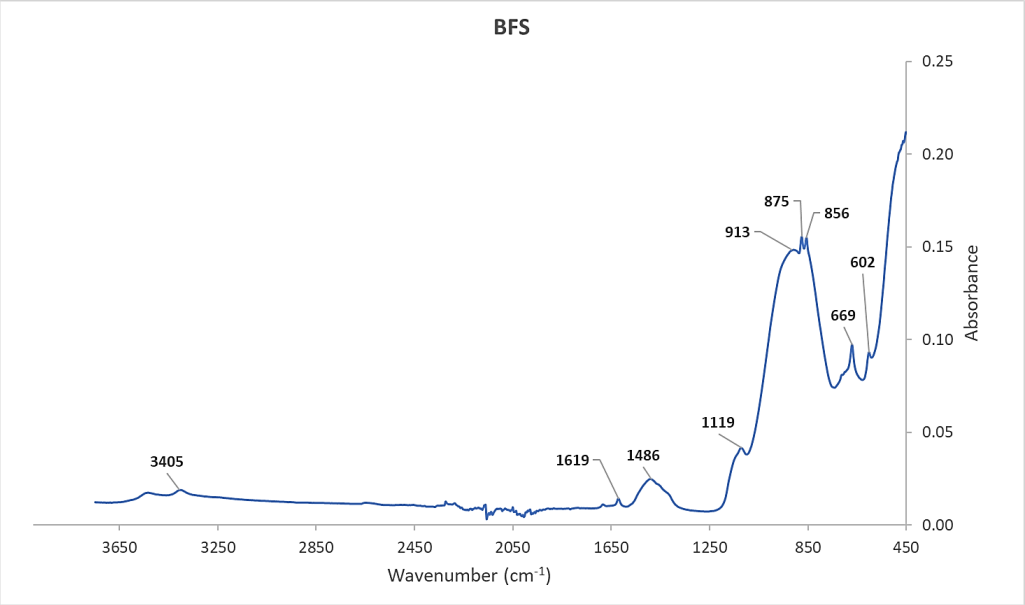

Figure S8. FTIR spectra of BFS.

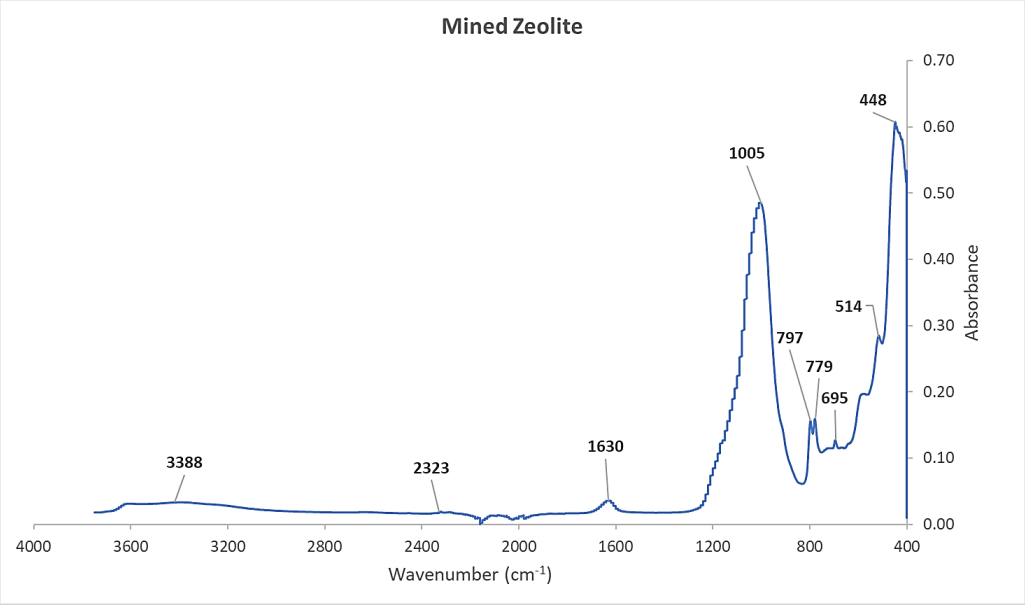

Figure S9. FTIR spectra of mined zeolite.

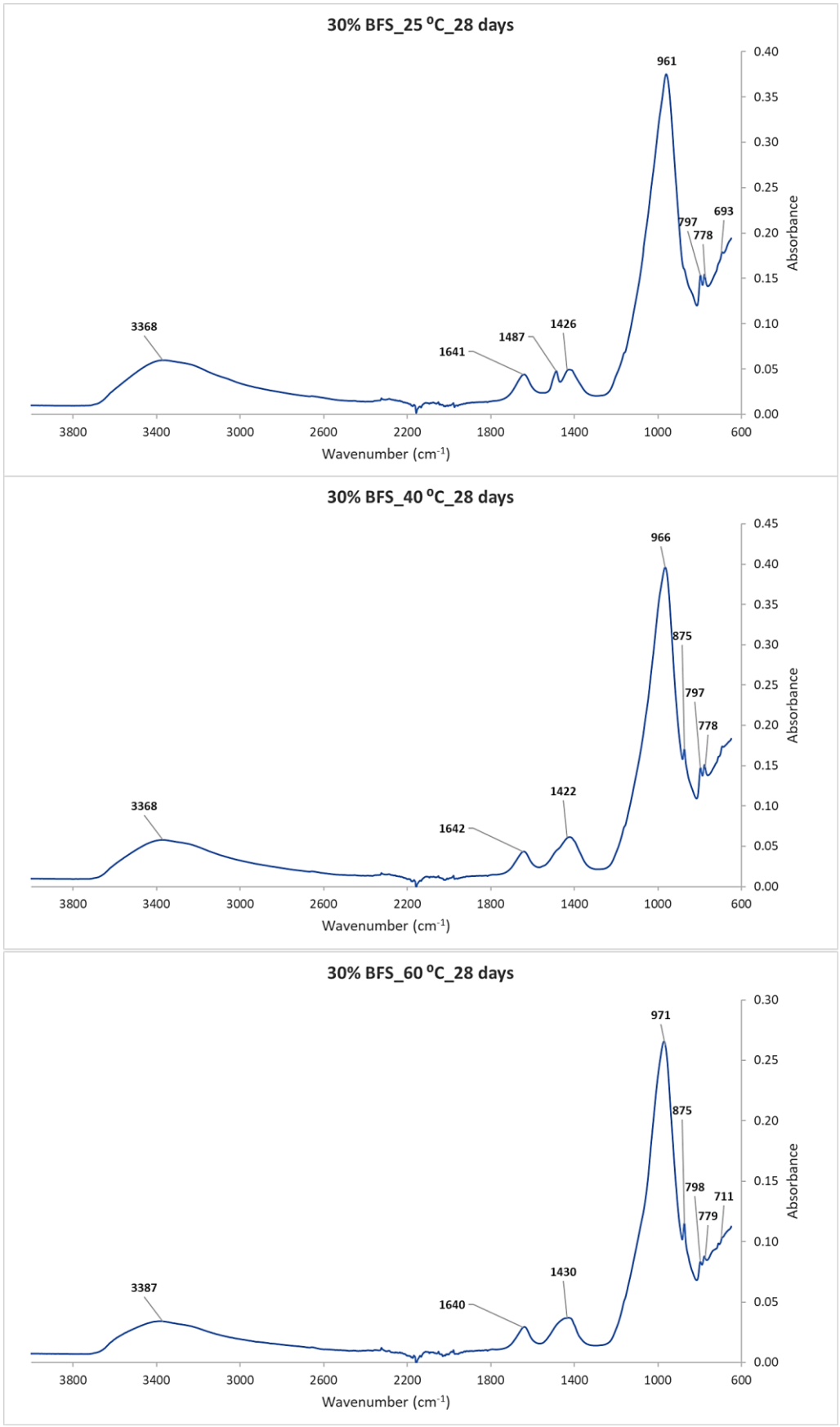

Figure S10. FTIR spectra: Geopolymer samples with 30% BFS cure at different temperatures.